Materials Chemistry and Physics 169 (2016) 55–61

Contents lists available at ScienceDirect

Materials Chemistry and Physics

journal homepage: www.elsevier.com/locate/matchemphys

Chemical, physical, and mechanical properties evolution in electron beam irradiated isotactic polypropylene

Eduardo A. Maeda [a], Alessandra F. Santos [b], Leonardo G.A. Silva [c], Cláudio G. Schön [d, *]

[a] Centro Universitário Nove de Julho, Av. Dr. Adolpho Pinto, 109, CEP 01156 – 050 São Paulo, Brazil
[b] Faculdade de Tecnologia de Mauá, Centro Estadual de Educação Tecnológica "Paula Souza", Av. Antônia Rosa Fioravante, 804, CEP 09390-120 Mauá, Brazil
[c] Instituto de Pesquisas Energéticas e Nucleares, Comissão Nacional de Energia Nuclear, Av. Prof. Lineu Prestes, 2242, CEP 05508-000 São Paulo, Brazil
[d] Dept. Metall. Mater. Engineering, Escola Politécnica da Universidade de São Paulo, Av. Prof. Mello Moraes, 2463, CEP 05508-030 São Paulo, Brazil

HIGHLIGHTS

- Instrumented indentation results do not correlate with the tensile results.
- Young modulus shows a large decrease for irradiation above 100 kGy.
- UV–VIS shows that degradation is continuous, by production of chromophores.
- XRD shows initially amorphization, but crystallinity is recovered above 100 kGy.

ARTICLE INFO

Article history:
Received 17 July 2015
Received in revised form
17 November 2015
Accepted 20 November 2015
Available online 2 December 2015

Keywords:
Polymers
Compaction
Hardness
Irradiation effects
Visible and ultraviolet spectrometers
Recrystallization

ABSTRACT

Isotactic Polypropylene 3 mm thick tensile samples, prepared by compression molding, were subject to electron beam irradiation with doses 0, 20, 40, 60, 100, 200 and 300 kGy. These samples were characterized by spectroscopic methods (UV spectroscopy), X-ray diffraction and mechanical tests (tensile tests and instrumented indentation), with the aim to investigate the ability of the instrumented indentation test to detect the changes in the macroscopic properties which arise from the changes in the chain structure. The use of larger irradiation doses compared with the commercial levels led to an unexpected behavior. At the smaller doses (up to 60 kGy), as expected, sample crystallinity decreases, characterizing irradiation induced amorphization. For the 100 kGy dose, however, the sample recrystallizes, returning to crystal/amorphous phase ratios similar to the ones observed for the pristine material. These changes correlated with the progressive production of –C═O and –C═C– chromophores in the chain and with a loss in yield strength and Young modulus up to 200 kGy (the sample subjected to 300 kGy is brittle). In spite of this, the indentation test showed limited sensitivity to the changes in the macroscopic tensile properties.

1. Introduction

Instrumented indentation has been in use already for several decades, as a technique to probe mechanical properties of small volumes of materials [1,2]. In metals, in which the technique was first applied, the technique allows to probe several macroscopic properties, like hardness, Young modulus, yield strength, strain hardening exponent, among others [3,4].

There are, of course several works which deal with the extraction of macroscopic mechanical properties from instrumented indentation data in polymers [5–12], the algorithms, however, are more complex than those used for metals and alloys and sometimes the results are disappointing, showing no variation of the predicted mechanical properties, when large variations should be expected [7,8].

The primary aim of the present work is to report instrumented indentation data on an isotactic Polypropylene resin, as received and after electron beam irradiation. Since the main purpose was to test the mechanical properties, samples were extracted from compression molded plates and the samples themselves were subject to irradiation prior to testing. Electron beam irradiation alters the molecular structure of the polymer, hence these changes

* Corresponding author.
E-mail address: schoen@usp.br (C.G. Schön).

http://dx.doi.org/10.1016/j.matchemphys.2015.11.027
0254-0584/

have been monitored by chemical, spectroscopic and crystallographic methods.

2. Materials and methods

2.1. Material and samples

The resin employed in the present work is an isotactic Polypropylene (iPP) compounds, designated as HA722J, furnished by Nova Petroquímica (at the time, a division of Suzano Petroquímica SA, Mauá, Brazil). It is described as an iPP homopolymer with density between 0.89 and 0.91 g cm^{-3}, with high crystallinity, low fluidity and high stiffness, designed primarily for plastic parts injection molding. The material was furnished in granules of approximately 3 mm diameter. Melt flow index was measured, resulting in 0.35 ± 0.01 g $(10\ min)^{-1}$ [13].

The material was processed to obtain 3 mm thick compression molded specimens, according to ASTM Standard D4703 [14], using the flash mold configuration. Details of processing and additional specifications for the employed resin can be found in ref. [13]. The produced specimens were visually inspected, and found to be free of defects. The specimen geometry corresponded to dumbbell tensile specimens with dimensions according to class IV of ASTM standard D638 [15]. One set of samples was reserved for the investigation of the unirradiated material (pristine) and the remaining were subject to electron beam irradiation.

2.2. Electron beam irradiation

Sample irradiation was performed in Dynamitron Job 188 electron accelerator available at the Instituto de Pesquisas Energéticas e Nucleares (IPEN/CNEN-SP, Brazil). The irradiation settings are given in Table 1. Samples were placed in trays which were submitted to the electron beam at the prescribed speed. Total dose was obtained by multiple passes under the beam (5 kGy per pass). Samples were submitted to doses of 20, 40, 60, 100, 200 and 300 kGy. These electron beam settings were designed to warrant full penetration in the 3 mm, so that a gradient is expected to exist along the sample's thickness, but the applied dose is the same on both sides and constant through the whole section [16].

Polymer irradiation under air, at room temperature, may result in trapped charges and radicals, which lead to post-treatment reactions, particularly due to the constant supply of oxygen. Mowery et al. [17], for example, investigated these reactions after γ irradiation of PP using ^{13}C Nuclear Magnetic Resonance (NMR). These authors reported linear or logarithmic kinetics for these reaction in a timespan of 700 days. On similar grounds, Fel et al. [18] recently investigated γ irradiation of PP and PE using Electron Paramagnetic Resonance (EPR). These authors focused on the signal arising from trapped radicals in the samples and report a time constant of ca. 73 h for decay of alkylperoxyl (O_2) radicals in PP as the most time resilient process. Neither the radical decay products, nor the time dependent reactions were characterized in the present work, but tests were performed as close as possible from irradiation, not superseding 40 h after the irradiation. This period, assuming Mowery et al. [17] results could be extrapolated to represent the present case, is insufficient for the occurrence of appreciable changes in the polymer matrix. The only exception to this rule was observed in the X-ray diffraction experiments, which, due to technical reason, could be performed only one month (30 days) after irradiation. Results of some preliminary tests performed just after irradiation, however, were indistinguishable from the ones presented here, therefore they are believed to be representative.

As stated before, the irradiation settings were chosen such that most electrons have enough energy to trespass the cross section of the sample, even after a few collision events. Some of these electrons, however, may perform multiple collision events in the matrix, loosing enough energy to become trapped as free charges. It is expected that the density of such trapped charges will be greater for the higher doses, but the present authors consider that this density is sufficiently low, not affecting the results.

Table 1
Settings for the electron accelerator.

Parameter	Value
Beam energy	1.103 MeV
Beam width/scan	100 cm
Beam current	4.74 mA
Tray speed	6.72 m min^{-1}
Dose rate	23.39 kGy s^{-1}

2.3. Tensile tests

Mechanical tests were conducted in an electromechanical universal testing machine, using a calibrated 1 kN load cell. Ten specimens were tested for each condition. Samples were tested under displacement control, with crossbar displacement set at 50 mm min^{-1}. No extensometer was used in the present tests. Ten specimens were tested for each condition.

Fracture surfaces in selected samples were observed using a XL30 Phillips electron microscope. Images were produced in the secondary electron mode, using 20 kV acceleration in gold sputtered surfaces.

2.4. Instrumented indentation

Instrumented indentation tests were performed in a Fischerscope H100V microindenter, available at the Laboratório de Fenômenos Superficiais (LFS) of the Escola Politécnica da USP, using a Vickers diamond pyramidal indenter. The maximum load (P_{max}) was set to 150 mN. Load, P was registered as a function of the instantaneous penetration depth, h, in a loading/holding/unloading cycle. The loading portion was set to 30 s, with acquisition time of 0.5 s (i.e. 60 points in the loading curve). The load was kept at its maximum value for 20 and 60 s (respectively 40 and 120 acquisition points) and the unloading portion took 50 s (100 acquisition points).

Samples were prepared for the indentation tests by grinding (using 220, 320, 400, 600, 1000 and 4000 mesh SiC paper) and polishing in metallographic cloth (without adding diamond paste) using detergent as lubricant. This procedure was found to produce acceptable surfaces for the indentation tests. Ten measurements were made in each sample.

Results are evaluated in terms of the universal hardness, HU, defined as:

$$HU = \frac{P_{max}}{A(h_{max})} \tag{1}$$

where h_{max} is the maximum penetration depth (the penetration depth at maximum load) and $A(h) = 24.5h^2 + 4.7372h - 2.34786\sqrt{h}$ is the contact area. This expression of $A(h)$ is calibrated for the Vickers indenter used in the LFS.

A second parameter is the Young modulus, E, estimated using the expression:

$$E_r = \frac{\sqrt{\pi}}{2\beta}\frac{S}{\sqrt{A(h_c)}} \quad (2)$$

where $\beta = 1.034$ is a form factor for the Vickers indenter, $S = \frac{dP}{dh}|_{h_{max}}$, is the contact stiffness, and, E_r is the reduced Young modulus of the system indenter + sample, which is postulated to be defined as [1,2]:

$$\frac{1}{E_r} = \frac{(1-\nu^2)}{E} + \frac{(1-\nu_i^2)}{E_i} \quad (3)$$

with $E_i = 1029$ MPa and $\nu_i = 0.07$ being respectively the Young modulus and Poisson coefficient of the indenter material (diamond) [19] and $\nu = 0.38$ being the Poisson coefficient of the resin (estimated).

2.5. Structure characterization

2.5.1. Chain structure

The changes in the chain structure, caused by irradiation, were characterized by ultraviolet–visible spectroscopy (UV–VIS) and by chemical methods.

The UV–VIS spectra were acquired in absorption mode using a Cary 50 Conc UV–Visible spectrophotometer. The samples were analyzed through the original thickness (3 mm), so that no special preparation was needed.

Additionally, the samples were dissolved in boiling xylene to investigate the fraction of chains affected by irradiation induced crosslinking. The method of Soxhlet extracting with xylene was used to determine the level of gel for each sample at 132 °C during 24 h. After that, samples with mass around 0.3 g were washed and dried in an oven at 80 °C. The gel fraction was calculated when the sample reached constant mass.

2.5.2. X-ray diffraction

X-ray diffraction experiments were made in 25 × 25 mm samples cut out of the heads of the tensile specimens, using a Rigaku Multiflex diffractometer, operating with a copper tube (CuKα radiation, $\lambda = 0.154184$ nm, operating at 40 kV and 20 mA). Patterns were acquired in the θ–2θ geometry, with parallel beams in the $3° \leq 2\theta \leq 90°$, with 0.2° step.

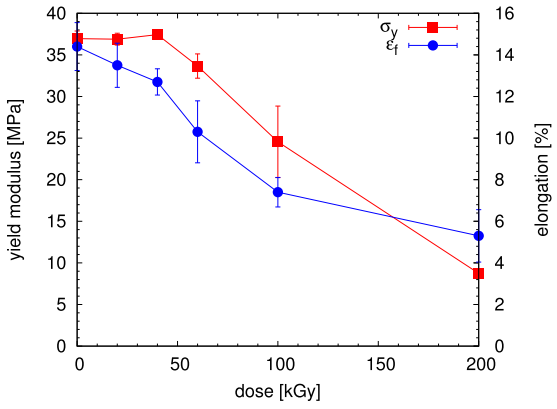

Fig. 1. Results of the tensile tests (reported values are averages of 10 specimens and bar height corresponds to the standard deviation).

3. Results and discussion

3.1. Mechanical behavior

Fig. 1 summarizes the results of the tensile tests in the pristine and irradiated samples. The values for the 300 kGy irradiated sample are not included, because this material, consistently, fractured in a brittle mode with negligible load.

The results shows a picture consistent with a continuous irradiation-induced degradation, which is more evident in the elongation results, but is also observed in the yield strength data for samples irradiated beyond 60 kGy. The brittle behavior of the 300 kGy samples can be justified by the results of the boiling xylene dissolution, since this is the only case in which an appreciable degree of crosslinking (4.32%) is observed.

These values are consistent with results from the literature. Manas et al. [20], for example, investigated electron beam irradiation of iPP, with the addition of a crosslinking agent, which is activated by the electrons. These authors show a moderate increase of Young modulus and tensile strength and a decrease in impact energy for doses up to 33 kGy, which is consistent with the present findings (assuming impact energy correlates with the elongation, whose values are not reported by the authors). A moderate decrease of strength and a large decrease of elongation (or impact energy) in PP with electron beam irradiation were also reported by Riquet et al. [21], at a dose of 100 kGy, and by Alfaro et al. [22], at doses up to 500 kGy. Similar results are observed in Polyamide 6 (PA6) irradiation with electron beam [23].

Fig. 2 presents the results derived from the indentation tests using Equations (1) and (2). The values for the Young modulus (Fig. 2(a)) show a drastic difference of behavior for the resin when irradiated below and above 100 kGy. At lower doses, the modulus slightly increases with dose, but a sharp transition is observed at 100 kGy, and the modulus decreases to values about half the ones observed for the pristine resin. Values of universal hardness (HU), (Fig. 2(b)), on the other hand, show almost no variation with irradiation dose. In both cases, the results obtained in the indentation tests and in the macroscopic tensile tests cannot be reconciled.

Manas et al. [20] also investigated electron beam irradiation of iPP by instrumented indentation with doses up to 33 kGy. These results are compatible with the ones shown in Fig. 2.

3.2. Fracture surfaces

Fig. 3 shows the fracture surface appearance of selected tensile samples corresponding to the prescribed irradiation doses. The pristine sample and the irradiated samples up to 60 kGy show a rough fracture surface which resemble hackle marks. In some of the sample (for instance, in the pristine and in the 20 kGy sample) small mirror areas are found close to the upper left corner of the images. The 100 kGy sample is a particular case. The fracture surface is divided in two portions, one which resemble the samples corresponding to lower doses and a smoother one. For higher doses, the smooth aspect of the fracture surface prevails.

Fig. 4 shows fracture surfaces of the pristine and for the 60 kGy irradiated samples with a higher magnification. These are representative of the samples which were irradiated up to this dose. Both images show features which resemble “scales”, suggesting the main crack was followed by profuse branching and tearing of plane fibril-like features. Dasari et al. [24] denominate this morphology “crazing-tearing” and attribute its formation to the nucleation of crazes and the subsequent tearing of the fibrils. Similar morphologies have also been identified in conventionally processed iPP, independent of microstructure [25]. The directionality of these “scales” is also similar in both images and this shows that, up to this

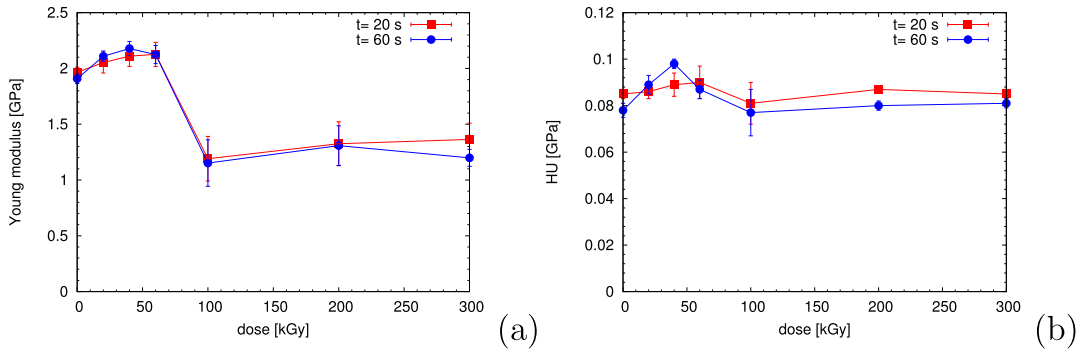

Fig. 2. Results of the indentation tests (reported values are averages of 10 specimens and bar height corresponds to the standard deviation). Young modulus (a) and Universal hardness (b) as function of irradiation dose.

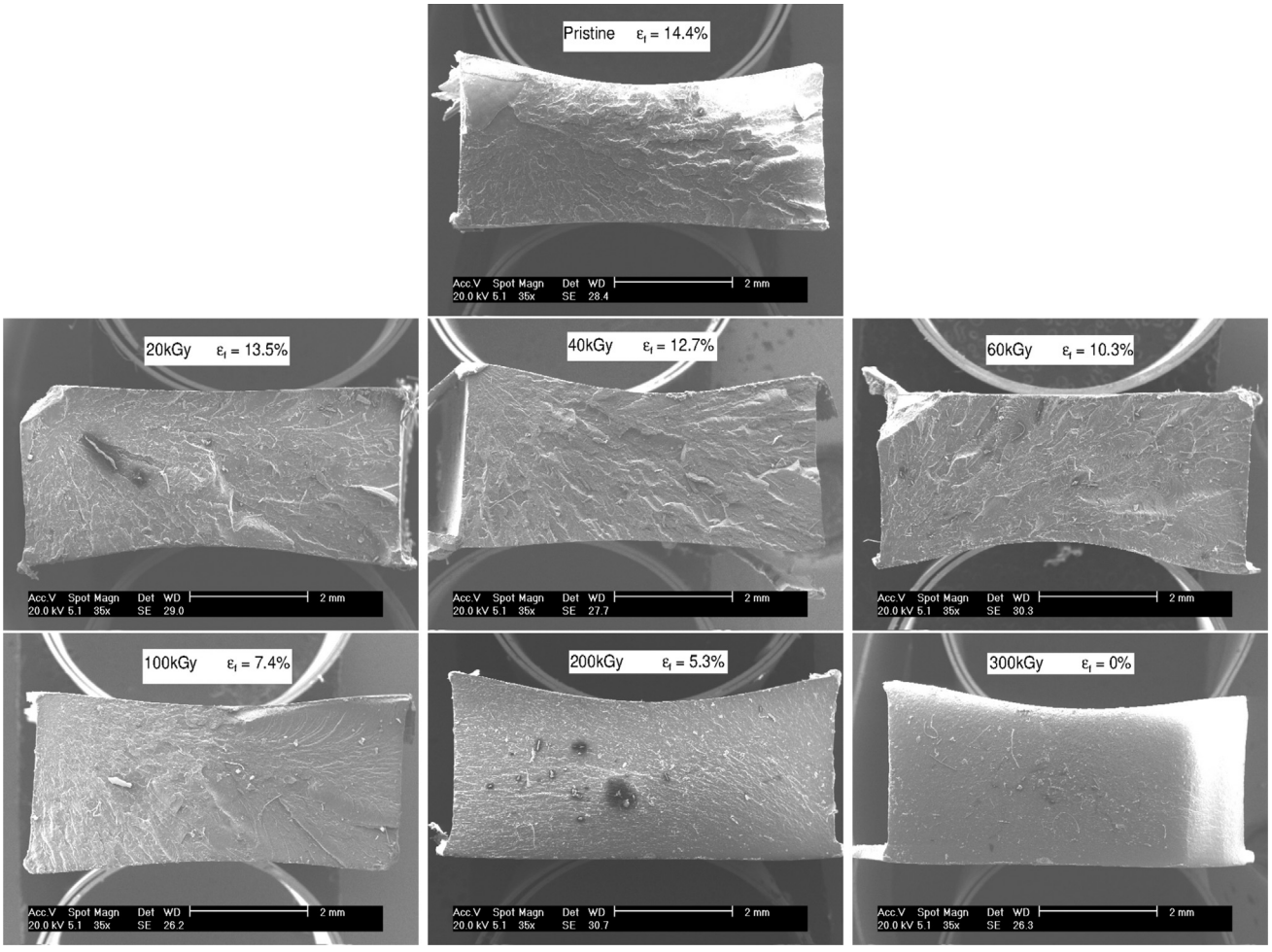

Fig. 3. Fracture surface appearance in selected tensile samples corresponding to irradiation doses and average elongation indicated in the images.

point, the basic fracture mechanism did not change in spite of the decrease in ductility.

This situation starts to change in the sample with irradiated for a dose of 100 kGy (Fig. 5). The rough side of the fracture surface (Fig. 5(a)) is similar to the ones observed in Fig. 4, but the smooth side (Fig. 5(b)) shows more continuous scales, suggesting crack branching becomes coarser and less profuse.

This transition to a less branched cracking completes for the 200 kGy, Fig. 6(a), and 300 kGy samples, Fig. 6(b). In the case of the 200 kGy sample, we observe long continuous features which are related to the scales observed with smaller doses. It is observed that crack branching, in this case, became less effective, with smaller secondary cracks. The crack branching at sample irradiated at the 300 kGy dose is practically non existing and are reduced to rare events in the fracture surface, which shows only an undulated smooth surface. This morphology is close to the “brittle” mechanism, identified by Dasari et al. [26].

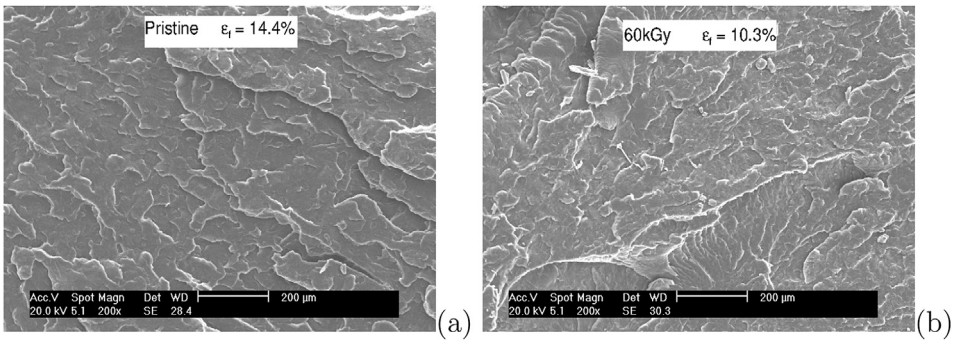

Fig. 4. Detail of the samples: (a) pristine, $\varepsilon_f = 14.4\%$ and (b) irradiated with 60 kGy, $\varepsilon_f = 10.3\%$.

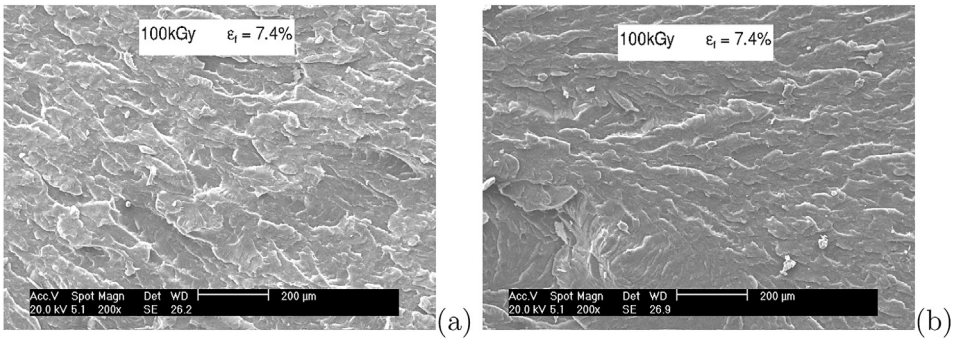

Fig. 5. Detail of the sample irradiated at 100 kGy dose ($\varepsilon_f = 7.4\%$), (a) rough side of the fracture surface and (b) smooth side of the fracture surface.

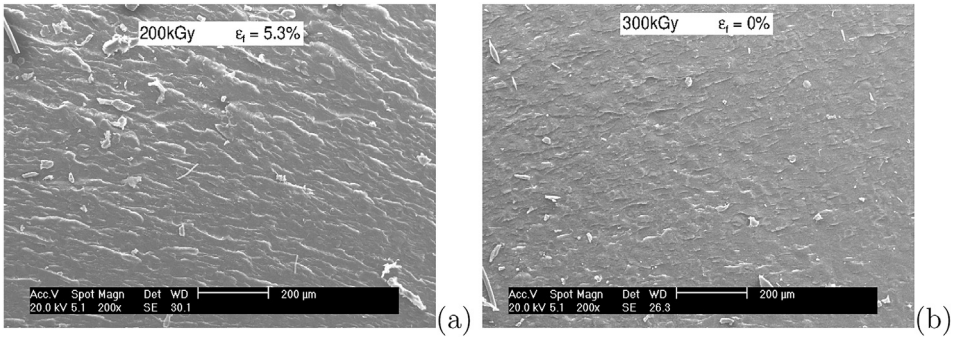

Fig. 6. Detail of the samples: (a) irradiated with 200 kGy dose, $\varepsilon_f = 5.3\%$ and (b) irradiated with 300 kGy dose, $\varepsilon_f = 0\%$.

3.3. Structural changes

Fig. 7 presents the UV–VIS spectra of the pristine and irradiated specimens. The pristine polymer presents a natural absorption peak around $\lambda = 195$ nm. With irradiation (up to 60 kGy) the continuous development of a band around 190–222 nm is observed. The formation of this band and its broadening with irradiation is usually attributed to development of chromophore groups (dienes) in the chain. At higher doses (above 100 kGy) an additional contribution around 222 and 270 nm is observed, which is usually attributed to the formation of triene. The picture of irradiation damage is completed by the development of a sharp peak around 195 nm (superposed to the previously described diene contribution), which is attributed to the formation of carbonyl groups in the chain [27]. The development of these contributions in the UV–VIS spectra correlates with a visual alteration of color in the specimens (yellowing) [13].

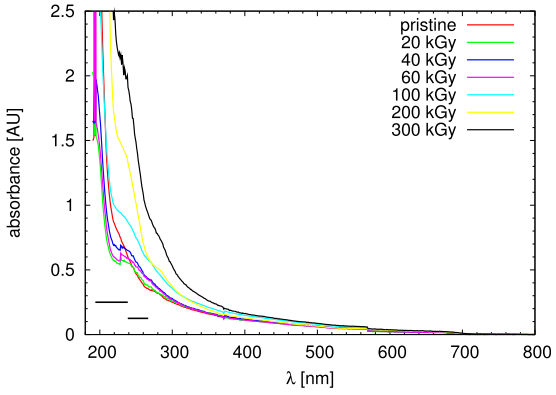

Fig. 7. UV–VIS spectra of the pristine and irradiated specimens.

Oka et al. [28] also observed the continuous formation of diene groups in the chain of iPP submitted to ion beam irradiation. Alfaro et al. [22] and Abraham et al. [29] identify the formation of carbonyl groups in iPP submitted to electron beam irradiation with doses up to 500 kGy. Irradiation induced crosslinking is also observed by several authors in PP by Oliani et al. [30] and by Manas et al. [20]. Similar results are obtained in Polyamide 6, submitted to electron beam irradiation [31] and in Polycyclooctene, submitted to γ irradiation [32].

Fig. 8 shows the results of the X-ray diffraction in the pristine and irradiated samples. Table 3 presents the corresponding calculated crystallinities. As observed, the behavior is distinct below and above 100 kGy. At first, electron beam irradiation continuously reduces crystallinity, characterizing radiation-induced amorphization. In the case of the 100 kGy sample, however, crystallinity reverts to values close to the ones observed in the pristine sample. Polypropylene is characterized by three polymorphs, one of which is known to be metastable. The possibility of radiation-induced phase transformation was investigated, but the reformed structure corresponds to the same existing in the pristine sample (the monoclinic α phase).

The possibility of attributing this recrystallization to the sample heating due to irradiation was considered, but previous experiments in the present instrument [33] concluded that a sample, with a density close to 1 g cm^{-3} had a temperature increase of 1 K when it absorbs a dose of 4.18 kGy. In the present work the samples were irradiated with electron beam in a conveyor with a speed of 6.72 m s^{-1}. For each pass under the electron beam sample absorbed a dose of 5 kGy, this corresponds to an increase in the temperature of 1.2 K. According to the route of the mat the samples pass almost simultaneously twice under the electron beam, increasing so the sample temperature by 2.4 K (assuming no heat loss in the process). Subsequent irradiation suffered from a delay of five minutes. This time was considered sufficient for the sample to return to room temperature. Therefore the temperature increase during irradiation is insufficient to justify the observed recrystallization.

Table 2 shows the lattice parameters estimated based on the linear regression using the peak positions (only samples which possessed enough reflections were analyzed). Above 100 kGy, the crystallinity decreases again, but the material seems to stabilize at a crystallinity level slightly above 10%. This strange behavior is subject of an ongoing investigation, but it clearly correlates with the large drop in Young modulus (Fig. 2(a)), showing it is probably linked to a reduction in strength of the secondary (interchain) bonds.

Several authors [21,22,34] report a continuous, but modest decrease of crystallinity for polymers submitted to irradiation with

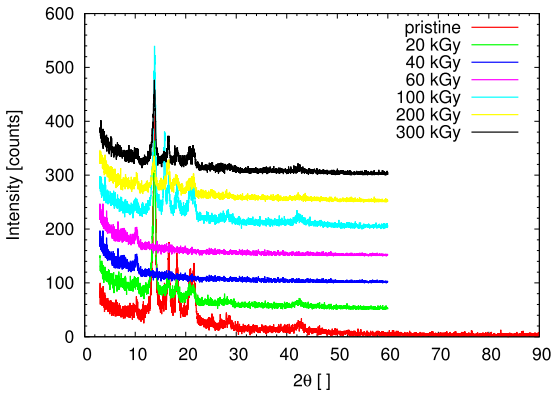

Fig. 8. X-ray diffractograms of the pristine and irradiated samples.

Table 2
Lattice parameters of the α iPP phase.

Dose	a (nm)	b (nm)	c (nm)	β (degrees)
Pristine	0.681	2.100	0.656	99.0
20 kGy	0.680	2.134	0.664	99.3
100 kGy	0.670	2.182	0.656	98.5
200 kGy	0.681	2.146	0.655	98.9
300 kGy	0.676	2.137	0.664	98.7

electron beam, using doses up to 500 kGy. A reversion to the crystalline state, however, has not been previously reported. One possible explanation for this inconsistency would be that all these authors estimate crystallinity through Differential Scanning Calorimetry (DSC). Supposing the amorphous state is metastable, with a low activation barrier for reversion, it would be reasonable to suppose that this reversion would happen during the heating already in the first DSC run. Our results are direct measures of the crystalline phase at the irradiation temperature (room temperature).

Linggawati et al. [35] investigated the electron beam irradiation of Nylon-66 membranes produced with organic and inorganic additives. These authors observed, for some investigated conditions, an enhancement of intensity in diffraction peaks (hence, of the crystallinity) which where attributed to the interaction with the additives. Abdel-Salam et al. [36] investigated proton irradiation of a polycarbonate resin and also identified an increase in crystallinity for a limited proton fluence interval and attributed this effect to degradation, which would reduce the number of entanglement points in the polymer, resulting in increased chain mobility. Polycarbonate is know for its low natural crystallinity, which is probably the reason why these authors only observed an irradiation enhancement of the crystalline fraction. A similar model, however, could be adapted to explain the present results, with a competition of the degradation effect, first destroying the crystalline regions, but later, increasing the chain mobility, after a critical number of entanglement points have been affected, leading to a recovery of the crystallinity. This picture is also consistent with the large drop in Modulus values observed in our samples with doses above 100 kGy by the indentation test.

4. Conclusions

In the present work, samples of an isotactic Polypropylene resin were subject to electron beam irradiation, in order to obtain large variations in mechanical properties in relatively chemically similar polymers. Naturally the chain structure changes with irradiation, but these modifications are small and continuous, such that most of the polymer matrix remain unaltered. The obtained results showed that electron beam irradiation leads to degradation as evidenced by the tensile results: both strength and ductility decrease with increasing dose.

The materials were, then, investigated by instrumented indentation. It is unlikely that the results of Young modulus and Hardness could correlate with the macroscopic property changes. The technique is sensitive enough to detect a large change in properties for the samples which were irradiated with doses above 100 kGy (in the Young modulus data).

Irradiation induces changes in the chemical structure of the polymer, producing chromophores (dienes, trienes and carbonyl groups). These changes are cumulative. However, these changes are continuous and cannot justify the large change in Young modulus for samples irradiated with doses above 100 kGy.

The X-ray diffraction data show that, initially, irradiation induces amorphization, but this amorphization is reverted for the

Table 3
Calculated crystallinities of the pristine and irradiated samples.

Sample	Pristine	20 kGy	40 kGy	60 kGy	100 kGy	200 kGy	300 kGy
Crystallinity	21%	19%	11%	12%	21%	15%	17%

100 kGy dose, which correlates with the large reduction in the Young modulus data.

Acknowledgments

The authors would like to thank Prof. Roberto M. Souza (Escola Politécnica, University of São Paulo) and Prof. Yoshio Kawano (Instituto de Química, University of São Paulo) for useful discussions. This work has been financially supported by the Brazilian National Research, Development and Innovation Council (CNPq, Brasília, Brazil) (Proc. 312424/2013-2).

References

[1] M.F. Doerner, W.D. Nix, A method for interpreting depth-sensing indentation instrument, J. Mater. Res. 1 (1986) 601–609.
[2] W.C. Oliver, G.M. Pharr, An improved technique for the determination of hardness and elastic modulus using load and displacement sensing indentation experiments, J. Mater. Res. 7 (1992) 1564–1583.
[3] A.E. Giannakopoulos, S. Suresh, Determination of elastoplastic properties by instrumented sharp indentation, Scr. Mater. 40 (1999) 1191–1198.
[4] G. Pintaúde, M.G.V. Cuppari, C.G. Schön, A. Sinatora, R.M. Souza, A review on the reverse analysis for the extraction of mechanical properties using instrumented Vickers indentation, Z. Met. 96 (2005) 1252–1255.
[5] M.R. VanLandingham, J.S. Villarubia, W.F. Guthrie, G.F. Meyers, Nanoindentation of polymers: an overview, Macromol. Symp. 167 (2001) 15–43.
[6] M.R. VanLandingham, Review of instrumented indentation, J. Res. NIST 108 (2003) 249–265.
[7] G.L.W. Cross, B.S. O'Connel, J.B. Pethica, H. Schulz, H.-C. Scheer, Instrumented indentation testing for local characterization of polymer properties after nanoprint, Microelectron. Eng. 78 – 79 (2005) 618–624.
[8] A.F. Santos, H. Wiebeck, R.M. Souza, C.G. Schön, Instrumented indentation testing of an epoxy adhesive used in automobile body assembly, Polym. Test. 27 (2008) 632–637.
[9] J. Menčik, L.H. He, J. Němeček, Characterization of viscoelastic – plastic properties of solid polymers by instrumented indentation, Polym. Test. 30 (2011) 101–109.
[10] G. Peng, T. Zhang, Y. Feng, Y. Huan, Determination of shear creep compliance of linear viscoelastic – plastic solids by instrumented indentation, Polym. Test. 31 (2012) 1038–1044.
[11] G. Peng, Y. Feng, Y. Huan, T. Zhang, Characterization of the viscoelastic – plastic properties of UPVC by instrumental sharp indentation, Polym. Test. 32 (2013) 1358–1367.
[12] G.L. Oliveira, C.A. Costa, S.C.S. Teixeira, M.F. Costa, The use of nano- and micro-instrumented indentation tests to evaluate viscoelastic behavior of poly(-vinidilene fluoride) (PVDF), Polym. Test. 34 (2014) 10–16.
[13] A.F. Santos, Efeito da irradiação por feixe de elétrons sobre as propriedades físicas e químicas de uma resina de polipropileno, Ph.D. thesis, Escola Politécnica da Universidade de São Paulo, São Paulo, Brazil, 2011 (in Portuguese).
[14] ASTM Standard D4703, Standard Practice for Compression Molding Thermoplastic Materials into Test Specimens, Plaques or Sheets, ASTM International, West Cornshohocken, PA, 2010.
[15] ASTM standard D638, Standard Test Method for Tensile Properties of Plastics, ASTM International, 2010.
[16] S. L. Somessari, E. S. R. Somessari, C. G. Silveira, W. A. P. Calvo, Analysis of the power system from an electron beam accelerator and the correlation with the theoretical dosimetry for radiation processing, in: Proceeding of the International Conference on Development and Applications of Nuclear Technology (NUTECH-2014), Institute of Nuclear Chemistry and Technology (Warsaw).
[17] D.M. Mowery, R.A. Assink, D.K. Derzon, S.B. Klamo, R. Bernstein, R.L. Clough, Radiation oxidation of polypropylene: a solid-state ^{13}C NMR using selective isotopic labeling, Radiat. Phys. Chem. 76 (2007) 864–878.
[18] E. Fel, L. Khrouz, V. Massardier, L. Bonneviot, Comparative study of gamma-irradiated PP and PE polyolefins part 1: identification and quantification of radicals using electron paramagnetic ressonance, Polymer 77 (2015) 278–288.
[19] S.A.R. Pulecio, Modelamento do ensaio de indentação instrumentada usando elementos finitos e análise dimensional – análise de unicidade, variações experimentais, atrito e geometria do indentador, Ph.D. thesis, Escola Politécnica da Universidade de São Paulo, São Paulo, Brazil, 2010 (in Portuguese).
[20] D. Manas, M. Manas, L. Chvatalova, M. Stanek, M. Bednarik, A. Mizera, Effect of low doses beta irradiation on thermal, micro and macro mechanical properties of irradiated polypropylene, Radiat. Phys. Chem. 102 (2014) 171–177.
[21] A.-M. Riquet, J. Delattre, O. Vitrac, A. Guinault, Design of modified plastic surfaces for antimicrobial applications: impact of ionizing radiation on the physical and mechanical properties of polypropylene, Radiat. Phys. Chem. 91 (2013) 170–179.
[22] E.A. Alfaro, D.B. Dias, L.G.A. Silva, The study of ionizing radiation effects on polypropylene and husk ash composite, Radiat. Phys. Chem. 84 (2013) 163–165.
[23] E. Adem, G. Burillo, L.F. del Castillo, M. Vásquez, M. Avalos-Borja, A. Marcos-Fernández, Polyamide-6: the effects on mechanical and physicochemical properties by electron beam irradiation at different temperatures, Radiat. Phys. Chem. 97 (2014) 165–171.
[24] A. Dasari, J. Rohrmann, R.D.K. Misra, Microstructural aspects of surface deformation processes and fracture of tensile strained high isotactic polypropylene, Mater. Sci. Eng. A 358 (2003) 372–383.
[25] Q. Huan, S. Zhu, Y. Ma, J. Zhang, S. Zhang, X. Feng, K. Han, M. Yu, Markedly improving mechanical properties for isotactic polypropylene with large-size spherulites by pressure-induced flow processing, Polymer 54 (2013) 1177–1183.
[26] A. Dasari, J. Rohrmann, R.D.K. Misra, Microstructural evolution during tensile deformation of polypropylenes, Mater. Sci. Eng. A 351 (2003) 200–213.
[27] J. Workman, Handbook of Organic Compounds: NIR, IR, Raman, and UV-VIS Spectra Featuring Polymers and Surfactants, Academic Press, San Diego, 2001.
[28] T. Oka, A. Oshima, R. Motohashi, N. Seto, Y. Watanabe, R. Kobayashi, K. Saito, H. Kudo, T. Murakami, M. Washio, Y. Hama, Changes to the chemical structure of isotactic-polypropylene induced by ion-beam irradiation, Radiat. Phys. Chem. 80 (2011) 278–280.
[29] A.C. Abraham, M.A. Czayka, M.R. Fisch, Electron beam irradiations of polypropylene syringe barrels and the resulting physical and chemical property changes, Radiat. Phys. Chem. 79 (2010) 83–92.
[30] W.L. Oliani, D.F. Parra, H.G. Riella, L.F.C.P. Lima, A.P. Lugao, Polypropylene nanogel: "Myth or reality", Radiat. Phys. Chem. 81 (2012) 1460–1464.
[31] M. Porubská, I. Janigová, K. Jomová, I. Chodák, The effect of electron beam irradiation on properties of virgin and glass fiber-reinforced polyamide-6, Radiat. Phys. Chem. 102 (2014) 159–166.
[32] N. García-Huete, J.M. Laza, J.M. Cuevas, J.L. Vilas, E. Bilbao, J.M. León, Study of the effect of gamma irradiation on a commercial polycyclooctane I. Thermal and mechanical properties, Radiat. Phys. Chem. 102 (2014) 108–116.
[33] P.R. Rela, Desenvolvimento de um dispositivo de irradiação para tratamento de efluentes industriais com feixes de elétrons, Ph.D. thesis, Instituto de Pesquisas Energéticas e Nucleares (IPEN), São Paulo, Brazil, 2003 (in Portuguese).
[34] G. Burillo, E. Adem, E.M. Muñoz, M. Vásquez, Electron beam irradiated polyamide-6 at different temperatures, Radiat. Phys. Chem. 84 (2013) 140–144.
[35] A. Linggawati, A.W. Mohamad, C.P. Leo, Effect of APTEOS content and electron beam irradiation of physical and separation properties of hybrid nylon-66 membranes, Mater. Chem. Phys. 133 (2012) 110–117.
[36] M.H. Abdel-Salam, S.A. Nouh, Y.E. Radwan, S.S. Fouad, Structure and mechanical investigation of the effect of the effect of proton irradiation in Makrofol DE 7-2 polycarbonate, Mater. Chem. Phys. 127 (2011) 305–309.